

Cyclic Gait of A Novel One-legged Robot

Tao Geng Yupu Yang Xiaoming Xu

Laboratory of Intelligent Control, Department of Automation
A9903091, Shanghai Jiaotong University
Shanghai, 200030, P.R. CHINA

+86(21)-62932953

yngeng@263.net (or) yngeng@sina.com

Abstract

A novel construction of one-legged robot is proposed, which, unlike previous one-legged robot with springy legs, consists of three revolute joints, two links and two feet. On some conditions, it can be modeled as a two-degree-of-freedom manipulator. Inspired by our observation of a jumping frog, we design a cyclic gait for this one-legged robot. The gait is divided into four phases. During only two phases is active control exerted on the knee joint. The trajectory planning of the four phases is formulized as a problem of optimization subject to several constraints, including the ZMP constraint.

1. Introduction

1.1 One-legged robot

It is evident that legged locomotion is superior to wheeled locomotion on rugged terrain. By means of jumping or leaping, the animals and legged robots can easily negotiate some obstacles that may be impassible for the wheeled vehicles. Among the legged robots, the planar one-legged robots have absorbed many researchers due to the simplicity of its mechanical design. It was thought that the analysis and experiments of the one-legged robots may enlighten designing of the biped, quadruped and multi-legged robots. The first one-legged hopper built by Rabert [1] had a pneumatic cylinder installed in its leg and hence moved as a springy inverted pendulum while on the ground. Most of the one-legged robots proposed during the past two decades [7,8,9,10,11,12] were somewhat similar to Rabert's, since they all had some apparatus like a spring to restore energy and provide force for takeoff. As a result of such constructions, the well-established robot-

control theory (e.g., computed torque control) can not be effectively applied on these one-legged robots

The control strategy, adopted by Rabert [1], Pedro [7] and most of others, decouples the control problem of the one-legged hopper into three separate parts: hopping height control, forward speed control, and attitude control. Since the dynamic coupling effects becomes enormous in the case of large velocities, this strategy may not work perfectly on a fast locomotive robot. However, various control methods have been developed for the high-speed manipulators composed of revolute joints [6,14,15,16,]. Moreover, the technologies of driving and sensing of the revolute joints have been perfectly developed in the past years. Therefore, from an engineering viewpoint, we propose a one-legged locomotive robot which consists of revolute joints and may be able to take advantage of those control methods having been implemented successfully on high speed manipulators.

1.2 Model

Figure 2 is a sketch of the robot, which has three joints, two links and two feet. It is assumed that (1) the actuators and power sources are located at the three joints; (2) the four links are made of light sheet metal whose mass, compared with that of the joints, are negligible. Thus it is reasonable to simplify the robot as a model shown in figure 3. In figure 3, the three points of mass correspond to the three joints. The links and feet are massless.



Figure1. Snapshots of a jumping frog

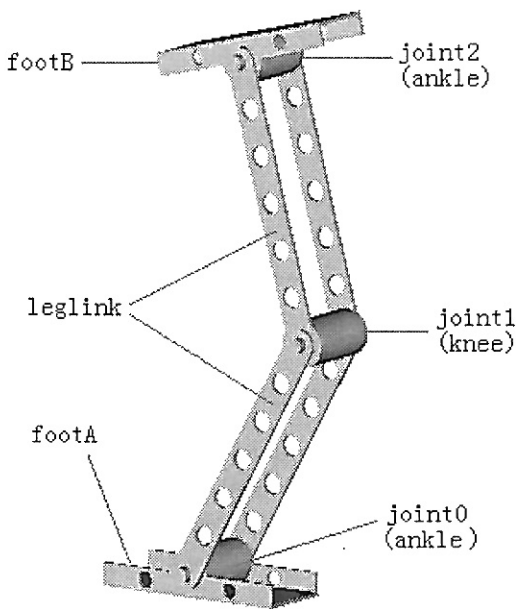


Figure 2. A sketch of the one-legged robot

1.3 Four phases of the cyclic gait

Observing of animals often illuminate robotics researchers. Jumping is the essential motion manner of frogs. Figure 1 is snapshots of a jumping frog during its flight phase. The trajectory of its center of mass (COM) is a ballistic curve, which is completely determined by the velocity of its COM at the instant of takeoff. There are no relative motions between its trunk and legs in flight phase, as if its hip and knee joints were “locked”. This strategy is economic, since internal motions don’t contribute to increasing the flight distance of its COM. However, the one-legged robots [11,12,13] had to regulate its attitude in flight phase, which was energy consuming and, unfortunately, didn’t increase the flight distance of the COM.

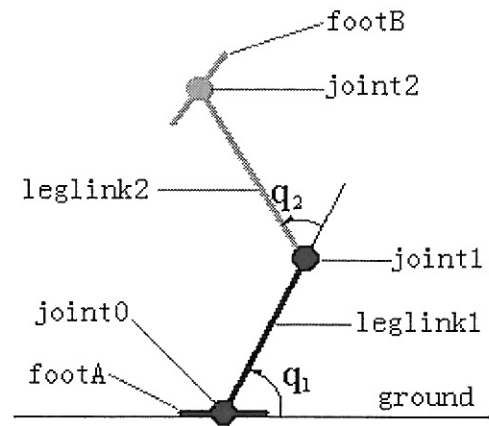


Figure 3. Model of the robot

Inspired by the jumping frog, we designed a cyclic jumping gait for our robot. A complete gait cycle is illustrated in figure 4. It is divided into four phases:

Phase 1. The time duration between the instant of landing of foot A and the instant of takeoff of foot A is phase 1. On some conditions, the robot can be seen as a manipulator during this phase.

Phase 2. This phase begins at the instant of takeoff of foot A, terminates at the instant of landing of foot B. It is assumed that, just after the instant of takeoff of foot A, the knee joint is locked by some mechanical apparatus. Just before the instant of landing of foot B, the knee joint is unlocked. In order to facilitate actualization of locking, the rotating rate of knee joint is specified to have just been decreased to be zero at the instant of takeoff. During this phase, rotational motion and translational motion decouple from each other. The trajectory of the COM is a ballistic curve. The three points of mass rotate about the COM at a fixed speed which is equal to the rotating speed of link 1 at the instant of takeoff.

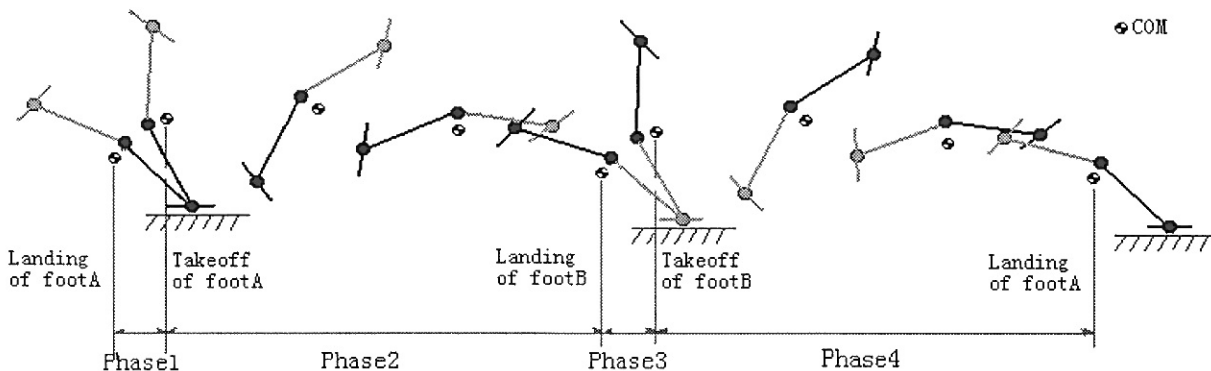


figure 4. A whole period of the cyclic gait

Phase 3. This phase is the same as phase 1, except for that foot A and foot B swap their roles.

Phase 4. This phase is the same as phase 2, except for that foot A and foot B swap their roles.

Noting that the first half of the cyclic gait (i.e., phase 1 and phase 2) and the second half have identical dynamics, we will only consider the first half. Since the links of feet have been assumed to be massless, so their motions have no effects on the dynamics of the robot. Consequently we will not consider the motion of the airborne foot, except for supposing that it has already been rotated to be parallel to the ground just before landing.

This paper is organized as follows: The second section addresses equations and constraints of phase 1 and 2. Then an optimal trajectory of locomotion is planned in the third section. Section 4 is some commentary.

Notations:

m Mass of each of the three joints.

$(x_1, y_1), (x_2, y_2), (x_c, y_c)$ Locations of joint 1, joint 2 and the COM, respectively.

$v_c = [v_{cx}, v_{cy}]^T$ Velocity of the COM.

$v_{1,landing}^-, v_{2,landing}^-, v_{c,landing}^-$ Velocities of joint 1, joint 2, and COM just before landing of foot A, respectively.

$v_{1,landing}^+, v_{2,landing}^+$ Velocities of joint 1 and joint 2 just before landing of foot A, respectively.

$q_{1,landing}^-, q_{2,landing}^-$ Angles of leg-link 1 and 2 just before landing of foot A, respectively. (see figure 5)

$q_{1,landing}^+, q_{2,landing}^+$ Angles of leg-link 1 and 2 just after landing of foot A, respectively. (see figure 5)

$t_{landing}^-, t_{landing}^+$ The time instants just before and just after landing of foot A, respectively.

ω_1, ω_2 Angular rates of leg-link 1 and 2, respectively. (see figure 3)

$x_{c,flight}, y_{c,flight}$ Location of the COM during flight phase, i.e., the phase 2.

$x_{c,takeoff}, y_{c,takeoff}$ Location of the COM at the

instant of takeoff of foot A.

T_f Duration of flight phase, i.e., the phase 2.

T Duration of phase 1.

2. Problem formulation

In this section, the motion equations and constraints of phase 1 and 2 are derived.

2.1 Phase 1: Foot A on the ground.

For convenience, we divide phase 1 into two time segments: $t_{landing}^- \sim t_{landing}^+$ and $t_{landing}^+ \sim t_{takeoff}$.

2.1.1 Landing of foot A

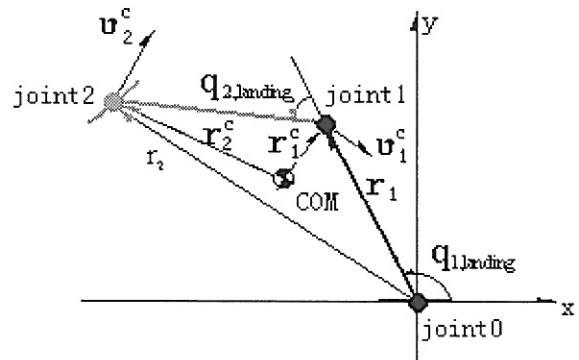


Figure 5. Landing of foot A

At landing, foot A hits the ground. As Goswami has done [2], we model the landing as an inelastic impulsive impact, which implies that (1) the angular momentum of the robot with respect to joint 0 (see figure 4) is conserved; (2) the angular momentum of joint 2 with respect to joint 1 is conserved.

According to this model of the impact, following equations can be derived:

$$m v_{1,landing}^- \times r_1 + m v_{2,landing}^- \times r_2 = m v_{1,landing}^+ \times r_1 + m v_{2,landing}^+ \times r_2 \quad (1)$$

$$m v_{2,landing}^- \times (r_2 - r_1) = m v_{2,landing}^+ \times (r_2 - r_1) \quad (2)$$

$$q_{1,landing}^- = q_{1,landing}^+ \quad (3)$$

$$q_{2,landing}^- = q_{2,landing}^+ \quad (4)$$

In figure 5, following equations can also be derived:

$$\mathbf{v}_{1, \text{landing}}^- = \mathbf{v}_{c, \text{landing}}^- + \mathbf{v}_{c_1}^c \quad (5)$$

$$\mathbf{v}_{2, \text{landing}}^- = \mathbf{v}_{c, \text{landing}}^- + \mathbf{v}_{c_2}^c \quad (6)$$

Where, $\mathbf{v}_{c_1}^c$, $\mathbf{v}_{c_2}^c$ are velocities of joint 1 and 2, relative to the COM.

Note that, at the time instant t_{landing}^- , (1) $\omega_{2, \text{landing}}^- = 0$; (2) joint 1 and 2 are rotating about the COM at a speed equal to $\omega_{1, \text{landing}}^-$. Thus the values of $\mathbf{v}_{c_1}^c$, $\mathbf{v}_{c_2}^c$ can be computed as

$$\mathbf{v}_{c_1}^c = \omega_{1, \text{landing}}^- \cdot \mathbf{r}_{c_1}^c \quad (7)$$

$$\mathbf{v}_{c_2}^c = \omega_{1, \text{landing}}^- \cdot \mathbf{r}_{c_2}^c \quad (8)$$

Considering equations (1)~(8), we can write

$$\begin{aligned} & [\omega_{1, \text{landing}}^+, \omega_{2, \text{landing}}^+]^T \\ &= \mathbf{H} [\omega_{1, \text{landing}}^-, \omega_{2, \text{landing}}^-]^T \end{aligned} \quad (9)$$

Where \mathbf{H} is a 2×2 matrix determined by the three parameters: $Q_{1, \text{landing}}^-$, $Q_{2, \text{landing}}^-$ and $\mathbf{v}_{c, \text{landing}}^-$

2.1.2 From the instant t_{landing}^+ to the instant of takeoff of foot A.

It is assumed that the friction coefficient is large enough to avoid sliding of foot A on the ground. Thus there are two constraints which must be satisfied during this time period:

(1) The vertical ground reaction force acting on the robot, N_y , must be positive, i.e., $N_y > 0$ (10)

$$N_y \text{ can be derived as } N_y = 3mg + m\ddot{y}_1 + m\ddot{y}_2 \quad (11)$$

(2) To describe the dynamic stability of locomotion and the physical admissibility of the gait, we adopt the concept of ZMP, which was first introduced by Vukobrtoric [3], and has been frequently used in the study of dynamical locomotion of bipedal robots.

The ZMP is defined as the point on the ground about which the sum of all the moments of active forces is equal to zero. If the ZMP is inside the contact polygon between the foot and the ground, the locomotion is dynamically stable [4]. In the case of our one-legged robot in the sagittal plane, the

ZMP condition is

$$|x_{\text{ZMP}}| < 0.5 \text{ footlength} \quad (12)$$

x_{ZMP} can be computed as:

$$x_{\text{ZMP}} = \frac{(\ddot{y}_1 + g)x_1 + (\ddot{y}_2 + g)x_2 - (\ddot{x}_1 y_1 + \ddot{x}_2 y_2)}{3g + \ddot{y}_1 + \ddot{y}_2} \quad (13)$$

On condition that the constraints formulated above have been satisfied, the one-legged robot can be seen as a manipulator during this time period. As a result, locomotion of the robot in this phase is to be simplified as a trajectory tracking problem of a two-degree-of-freedom manipulator.

By Lagrange's formulation [5], the dynamics equation of the two link rigid manipulator can be written as

$$\mathbf{D}(\mathbf{q})\ddot{\mathbf{q}} + \mathbf{C}(\mathbf{q}, \dot{\mathbf{q}}) + \mathbf{G}(\mathbf{q}) = \boldsymbol{\tau} \quad (14)$$

Where, $\mathbf{q} = [q_1, q_2]^T$, $\mathbf{D}(\mathbf{q})$ is the inertia matrix, $\mathbf{G}(\mathbf{q})$ is the gravity vector, $\boldsymbol{\tau}$ is the input torque vector, $\mathbf{C}(\mathbf{q}, \dot{\mathbf{q}})$ is the matrix of centripetal acceleration and Coriolis terms.

2.2 Phase 2: the flight phase

The condition for takeoff is that the vertical ground reaction force is zero, i.e., $N_{y, \text{takeoff}} = 0$ (15)

Considering what has been described about this phase in section 1.3, the trajectory of COM during this phase can be given as (see figure 6)

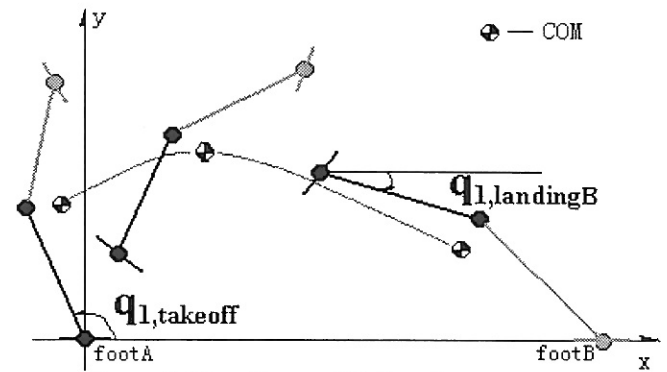


Figure6. The first flight phase

$$x_{c, \text{flight}} = v_{cx, \text{takeoff}} \cdot t \quad (16)$$

$$y_{c, \text{flight}} = y_{c, \text{takeoff}} + v_{cy, \text{takeoff}} \cdot t - 0.5gt^2 \quad (17)$$

According to the properties of this phase defined in section 1.3, the following equations are required:

$$q_{1,landingB} - q_{1,takeoff} = \omega_{1,takeoff} \cdot T_f \quad (18)$$

$$y_{c,landing} = y_{c,takeoff} + v_{cy,takeoff} \cdot T_f - 0.5gT_f^2 \quad (19)$$

$$\omega_{1,takeoff} = \omega_{1,landing}^- \quad (20)$$

Where, $q_{1,landingB}$ is the angular position of leg-link 1 at the instant of landing of foot B (see figure 6). It can be derived as

$$q_{1,landingB} = q_{1,landing}^- + q_{2,landing}^- - \pi \quad (21)$$

3. Trajectory planning

From equations (16) ~ (21), it can be deduced that the trajectory of phase 2 is completely determined by following four parameters:

$$v_{cx,takeoff}, v_{cy,takeoff}, q_{1,landing}^-, q_{2,landing}^-.$$

Therefore, we need only to plan the trajectory of phase 1.

We use time polynomial functions to describe the evolution of $q_1, q_2, \omega_1, \omega_2$, i.e.,

$$q_1(t) = a_4 t^4 + a_3 t^3 + a_2 t^2 + a_1 t + a_0 \quad (22)$$

$$q_2(t) = b_3 t^3 + b_2 t^2 + b_1 t + b_0 \quad (23)$$

$$\omega_1(t) = 4a_4 t^3 + 3a_3 t^2 + 2a_2 t + a_1 \quad (24)$$

$$\omega_2(t) = 3b_3 t^2 + 2b_2 t + b_1 \quad 0 \leq t \leq T \quad (25)$$

According to the equations in section 2, following constraints must be fulfilled:

$$q_1(0) = q_{1,landing}^+ \quad (26)$$

$$q_1(0) = q_{1,landing}^+ \quad (27)$$

$$\omega_1(0) = \omega_{1,landing}^+ \quad (28)$$

$$\omega_2(0) = \omega_{2,landing}^+ \quad (29)$$

$$q_1(T) = q_{1,takeoff} \quad (30)$$

$$q_2(T) = -q_{2,landing}^- \quad (31)$$

$$\omega_1(T) = \omega_{1,landing}^- \quad (32)$$

$$\omega_2(T) = 0 \quad (33)$$

$$N_{y,takeoff} = 0 \quad (34)$$

Considering equations (1) ~ (9) and equations (26) ~ (34), one can conclude that the polynomial functions (22) ~ (25) are uniquely defined by following four independent parameters:

$q_{1,landing}^-, q_{2,landing}^-, q_{1,takeoff}, T$, but these parameters must be chosen in order to ensure that the trajectories of q, \dot{q}, \ddot{q} satisfy the constraints (10) and (12). We solved this problem numerically by using the optimization algorithm *fmincon* in MATLAB.

The horizontal distance the COM travels during a complete gait cycle is selected as criteria in the optimization, which can be written as

$$C_{max} = 2(x_{c,takeoff} - x_{c,landing}^+ + v_{cx,takeoff} \cdot T_f)$$

To ensure the physical admissibility of the gait, in addition to constraints (10) and (12), finite angular rate and finite torque of the joints are taken into account as another two nonlinear constraints in the optimization. A simulation result is shown in figure 7.

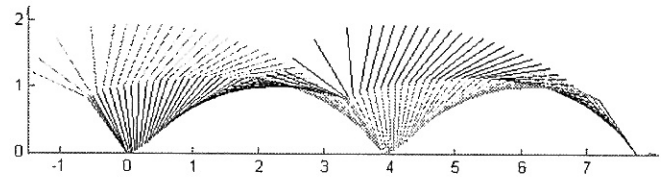


Figure 7. Stick diagram of an optimal cyclic gait (the two feet are omitted).

4. Commentary

Differing from other biologically inspired locomotive robots composed of complex artificial muscles or tendons, which were difficult to control, the one-legged robot proposed in this paper has a straightforward construction. Due to such a construction, the robot can initiate and stop autonomously. Its cyclic gait (figure 7) seems simple and graceful. Its primary disadvantage, compared with springy legged robots, is that the collision between its foot and ground is energy wasting. This problem may be

tackled by properly planning velocity of the foot before collision or adding springs to the joints, which will be considered in the future work.

References

- [1] Rabert, M.H., *Legged Robots That Balance*, MA: MIT Press, 1986.
- [2] Ambarish Goswami, A study of the Passive Gait of a Compass-like Biped Robot: Symmetry and Chaos, *Int. J. Robot. Res.* 17(12), 1998.
- [3] M. Vukobratovic and D. Juricic, Contribution to the synthesis of biped gait., *IEEE trans. On Bio-medical Engineering*, 16(1), 1969.
- [4] Qiang Huang, A High Stability, Smooth Walking Pattern for a Biped Robot, *Proceedings of IEEE International Conference of Robotics and Automation* 1999.
- [5] M.W.Spong and M. Vidyasagar, *Robot Dynamics and Control*, Wiley, New York, 1989.
- [6] Shiller Zvi and Chang Hai, Trajectory preshaping for high-speed articulated systems, *Journal of Dynamic Systems, Measurement and Control, Transactions of the ASME* 117 3 Sep 1995 ASME p 304-310.
- [7] Gregorio Pedro, Ahmadi Mojtaba and Buehler Martin, Design, control and energetics of an electrically actuated legged robot, *IEEE Transactions on Systems, Man, and Cybernetics, Part B: Cybernetics*, v 27, n 4 Aug 1997.
- [8] Saranli Uluc and Schwind William J., Toward the control of a multi-jointed, monopod runner, *IEEE International Conference on Robotics and Automation*, v 3, 1998
- [9] Okubo Hiroki, Nakano Eiji, Handa Minoru, Design of jumping machine using self-energizing spring, *IEEE International Conference on Intelligent Robots and Systems*, v 1, Nov 4-8, 1996.
- [10] Berkemeier Matthew D. Desai Kamal V. Design of a robot leg with elastic energy storage, comparison to biology, and preliminary experimental results, *IEEE International Conference on Robotics & Automation*, 1996
- [11] Lapshin V.V. Motion control of a legged machine in supportless phase of hopping, *International Journal of Robotics Research*, v 10, n 4, Aug 1991, p 327-337.
- [12] Francois Charles & Samson Claude, New approach to the control of the planar one-legged hopper, *International Journal of Robotics Research*, v 17, n 11 Nov 1998, Sage Sci Press, p 1150-1166.
- [13] Berkemeier M.D. Fearing R.S. Sliding and hopping gaits for the underactuated acrobot, *IEEE Transactions on Robotics and Automation*, v 14, n 4, Aug 1998.
- [14] Chitayev M.Y. Adaptive high-speed resonant robot, *Mechatronics*, v 6, n 8, Dec 1996, Elsevier Science Ltd, p 897-913.
- [15] Rastegar Jahangir S., Liu Lidong, Yin Dan, Task specific optimal simultaneous kinematic, dynamic, and control design of high-performance robotic systems, *IEEE/ASME Transactions on Mechatronics* Dec 1999, p 387-395
- [16] Youcef-Toumi K. and Kuo A.T.Y. High-speed trajectory control of a direct-drive manipulator, *IEEE Transactions on Robotics and Automation*, v 9 n 1, Feb 1993, p 102-108.